Diffraction-limited ultrasensitive molecular nano-arrays with singular nano-cone scattering

Yunshan Wang, Ting-Chou Chang, Paul R. Stoddart, and Hsueh-Chia Chang

Citation: Biomicrofluidics **8**, 021101 (2014); doi: 10.1063/1.4869694
View online: http://dx.doi.org/10.1063/1.4869694
View Table of Contents: http://scitation.aip.org/content/aip/journal/bmf/8/2?ver=pdfcov
Published by the AIP Publishing

Diffraction-limited ultrasensitive molecular nano-arrays with singular nano-cone scattering

Yunshan Wang,[1] Ting-Chou Chang,[1] Paul R. Stoddart,[2] and Hsueh-Chia Chang[1]
[1]*Department of Chemical and Biomolecular Engineering, University of Notre Dame, Notre Dame, Indiana 46556, USA*
[2]*Faculty of Science, Engineering and Technology, Swinburne University of Technology, Hawthorn, VIC 3122, Australia*

(Received 18 February 2014; accepted 15 March 2014; published online 26 March 2014)

Large-library fluorescent molecular arrays remain limited in sensitivity (1×10^6 molecules) and dynamic range due to background auto-fluorescence and scattering noise within a large (20–100 μm) fluorescent spot. We report an easily fabricated silica nano-cone array platform, with a detection limit of 100 molecules and a dynamic range that spans 6 decades, due to point (10 nm to 1 μm) illumination of preferentially absorbed tagged targets by singular scattering off wedged cones. Its fluorescent spot reaches diffraction-limited submicron dimensions, which are 10^4 times smaller in area than conventional microarrays, with comparable reduction in detection limit and amplification of dynamic range. © *2014 AIP Publishing LLC*. [http://dx.doi.org/10.1063/1.4869694]

Commercially available fluorescent micro-arrays based on target labeling, northern blot, or enzyme-linked immunosorbent assay (ELISA) are limited to a detection threshold of 1 to 10×10^6 molecules per fluorescent spot,[1–23] thus requiring cell culturing or Polymerase Chain Reaction (PCR) amplification for many applications. The low sensitivity is often due to broad illumination, which creates auto-fluorescence noise. Even if point illumination and pin-hole filtering of non-focal plane noise are implemented in a confocal setup, the large and non-uniform fluorescent spots create scattering noise over each 20–100 μm element, which degrades the detection limit.[4] Smaller spots can, in theory, be introduced by nano-sprays and nano-imprinting. However, directing the targets to such small areas then becomes problematic. Real-time PCR is, in principle, capable of detecting a single molecule but is limited in its target number[5] and is hence slow/ expensive for large-library assays. A large-library platform with much better detection limit than the current fluorescent microarrays would transform many screening assays. Ideally, this platform would not use the confocal configuration. Instead, it would direct the target molecules to a submicron spot and illuminate them with a nearby point source that does not require scanning.

A promising platform is the optical fiber bundle array,[6] with more than 10^4 fibers and targets, in principle. With its endoscopic configuration, these fiber bundles are most convenient for *in situ* and real-time biosensing modalities in microfluidic biochips and microfluidic 3-D cell cultures. Consequently, the optical sensing is typically carried out in the transmission mode, with the optical signals transmitted through the optical fibers to a detector. Microwell arrays at the distal end of imaging fiber, with molecular targets captured and transported to the microwells by microbeads, are the most popular among these optical fiber arrays. Although detection limit better than 1×10^6 molecules per bead has been reported, the bar-coded beads limit the target number of this platform.[7,8]

Our previous work[9,10] has shown that plasmonics at nanotips can enhance local electric field by three orders of magnitude. However, conduction loss and quenching of fluorescence[11,12] by the metal substrates limit the use of plasmonic enhanced fluorescence for large-library assays. Only nano-molar sensitivity has been demonstrated using plasmonics from metal coated nanocone tips.[13,14] In this paper, we will extend the conical fiber array platform not by tip

plasmonics but by another optical phenomenon with induced dipoles: singular scattering off dielectric wedges and tips.[15] Instead of the surface plasmon resonance on metallic nanostructures,[16] field focusing at the cone tip by the dielectric media (the silica fiber) is used to produce a localized and singularly large scattering intensity at the tip. Singular scattering from a wedge or a cone has been known for decades.[17,18] It is only recently that numerical simulation[19] has revealed that field focusing by this singular scattering can effect a five-order intensity enhancement that is frequency independent. This intense tip scattering produces a local light source at the tip that does not suffer from conduction loss. Unlike plasmonic metal nanostructures, the dielectric tip would also not quench the fluorescent reporters excited by the light source. In fact, it will help scatter the fluorescent signal, with Rayleigh scattering intensity scaling with respect to wavelength. We hence utilize this phenomenon for diffraction-limit fluorescent sensing/imaging for the first time here.

The local light source due to tip scattering minimizes background auto-fluorescence and scattering noise, provided the target molecules preferentially diffuse towards the dielectric vertices. If the targets do not preferentially hybridize with probes at the vertices, there would be significant target loss, with a concomitant loss in sensitivity, because the vertex regions are just a small fraction of the total area. Fortunately, like electromagnetic radiation at the electrostatic limit of the Maxwell equations for sharp (sub-wavelength) vertices,[20] the steady-state diffusion of molecules also obey the Laplace equation and so do the DC or AC electric potentials that drive electrophoresis and dielectrophoresis of the molecules.[21] Hence, the diffusive, electrophoretic, and dielectrophoretic fluxes of target molecules are also singularly large at the vertices and there will be preferential hybridization there until the tip is saturated. Previously, we have demonstrated preferential diffusive transport of colloids to channel corners[22] and dieletrophoretic trapping of bacteria[23] and DNA molecules[24] around sharp nanostructures like carbon nanotubes. Hence, dielectric nanotips fabricated by low-cost techniques can potentially provide the smallest fluorescent spot, which can preferentially capture target molecules and whose fluorescent image is limited in size only by the diffraction limit, without a confocal configuration.

Although the scattering singularity is stronger at the conic tip, the total increase in scattering area of this singularity of measure zero is not as high as that of a sharp wedge, thus rendering the signal relatively weak. We hence employ a well-defined multi-wedged silica cone fabricated by wet-etching, with the wedges introduced by non-uniform stress formed during the fiber assembly process, to produce maximum scattering at the tip where three to four wedges converge (see inset of Fig. 1(A)). Using the reflection mode to fully exploit this singular scattering to excite fluorescent reporters at the tip and transmit the resulting signal, we report a nanocone array that can detect down to 100 molecules per cone tip with a large dynamic range from femtomolar to nanomolar concentrations. Although quantification for a single target is reported in this preliminary report, multi-target assays can readily be developed.

Amine-modified 35-base oligo-probes were functionalized onto both unetched silica fibers (as a control) and etched conic silica tips. The sample of 35-base ssDNA targets (corresponding to a primer for a segment of the Serotype 2 dengue genome) with a 5′ tagged Cy3 fluorophore was inserted into a microfluidic chip housing the fiber bundle (Fig. 1(B)) and left overnight

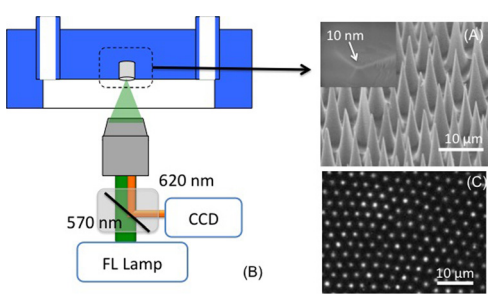

FIG. 1. (A) A SEM image of the silica cone array where the single cone inset image shows three wedges converging into a 10 nm junction at the tip. (B) The optical setup of measurement. (C) The diffraction-limited fluorescent spot images.

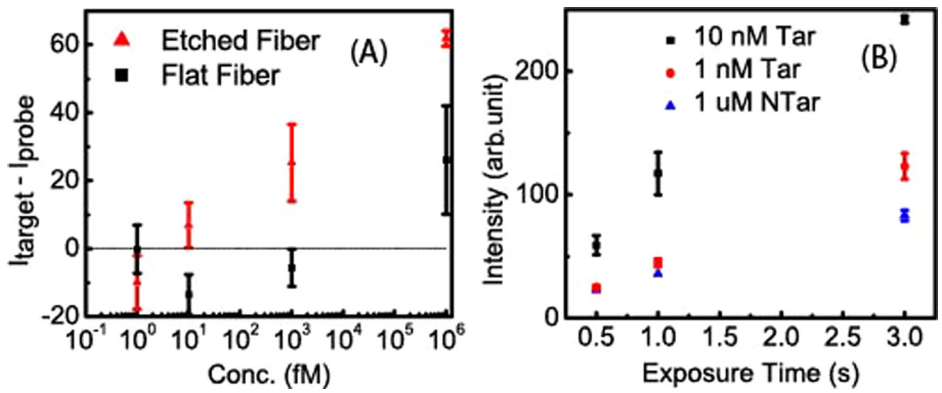

FIG. 2. (A) Fluorescent intensity of etched conic fiber and unetched fiber for different concentrations of target molecules from 1 fM to 1 nM. (B) Fluorescent intensity increases linearly with exposure time. Non-target molecules with 1 μM concentration do not produce significant signal compared to lower concentrations of target molecules such as 1 nM and 10 nM (see the supplementary material[25] for details of image analysis).

(see the supplementary material[25] for exact sequence). After a standard rinsing protocol, fluorescent images were taken with an Olympus IX-71 fluorescent microscope for target concentrations ranging from 1 fM to 1 nM. A typical fluorescent image after hybridization is shown in Fig. 1(c), where each micron-sized bright spot corresponds to a single tip in the cone array. The intensity profile shown in the supplementary material[25] indicates a fluorescent spot smaller than 1 μm, indicating that the fluorescent light source is sub-wavelength and the resolution is close to diffraction limit. The size of this bright spot at the conic tip does not vary much with respect to the concentration but its intensity does, as shown in Fig. 2(A). It was found that for flat fibers, only concentrations higher than 1 nM produced significant signals above the background. However, for etched conic fibers, 10 fM is clearly distinguishable from the background, which indicates that an improvement of sensitivity up to five orders can be realized by simply etching the flat surface into cone arrays. It also suggests very little target loss due to preferential hybridization onto the cone at sub-nM concentrations. We estimated the number of molecules per cone from the total number of molecules in target solution divided by the number of pixels on each fiber (10^4), which suggests less than 100 molecules per cone for a 10 fM bulk concentration, four orders better than any existing technology.

Selectivity of the platform was also examined. Fig. 2(B) presents the fluorescent intensity of the tips for non-target (1 μM) and target (1 nM and 10 nM) at different exposure times, which shows that fluorescent intensity increases linearly with exposure time. Beyond 5 s, saturation of images prevents further increase in the signal. For non-target, the intensity is much lower than 1 nM Target and 10 nM Target, which means non-target do not bind to the probes at the wedged tip as effectively as target molecules. Non-specific binding can be further removed by using more stringent buffers and higher flow rates.[26] This platform can be extended to detect 70 000 targets, in theory, by functionalizing different probes onto each cones using localized photochemistry via masking, micro-mirror directed illumination, or direct laser writing. Extension to ELISA type protein assays is also straight forward. Integration of a transmission-mode optical fiber endoscope into a microfluidic biochip and into a 3-D cell culture for real-time monitoring of multiple molecular targets at near-single molecule resolution is currently underway.

We thank S. Senapati, Z. Slouka, and Y. Yan of our lab for contributions to functionalizing the silica cones, fabricating the microfluidic chip and writing the image analysis software. This work is supported by NSF Grant No. CBET-1065652.

[1]S. Zhang, A. Garcia-D'Angeli, J. P. Brennan, and Q. Huo, Analyst **139**, 439 (2014).
[2]S. W. Kim, Z. Li, P. S. Moore, A. P. Monaghan, Y. Chang, M. Nichols, and B. John, Nucleic Acids Res. **38**, e98 (2010).
[3]J. Shingara, RNA **11**, 1461 (2005).

[4]See http://www.chem.agilent.com/library/applications/5988_9498en_scanner_paper72.pdf for the evidence of scattering noise degrading sensitivity of DNA microarray.
[5]D. Klein, Trends Mol. Med. **8**, 257 (2002).
[6]T. A. Dickinson, J. White, J. S. Kauer, and D. R. Walt, Nature **382**, 697 (1996).
[7]M. Bowden, L. Song, and D. R. Walt, Anal. Chem. **77**, 5583 (2005).
[8]F. Deiss, N. Sojic, D. J. White, and P. R. Stoddart, Anal. Bioanal. Chem. **396**, 53 (2010).
[9]Y. Wang, F. Plouraboue, and H.-C. Chang, Opt. Express **21**, 6609 (2013).
[10]Y. Wang, X. Cheng, and H.-C. Chang, AIChE J. **59**, 1830 (2013).
[11]N. A. Issa and R. Guckenberger, Opt. Express **15**, 12131 (2007).
[12]E. J. Sánchez, L. Novotny, and X. S. Xie, Phys. Rev. Lett. **82**, 4014 (1999).
[13]Y. Wang, S. Senapati, P. Stoddart, S. Howard, and H.-C. Chang, Proc. SPIE **8812**, 88120Q (2013).
[14]F. Deiss, S. Laurent, E. Descamps, T. Livache, and N. Sojic, Analyst **136**, 327 (2011).
[15]L. Cao, B. Nabet, and J. Spanier, Phys. Rev. Lett. **96**(15), 157402 (2006).
[16]S. Liu, Y. Yan, Y. Wang, S. Senapati, and H.-C. Chang, Biomicrofluidics **7**, 061102 (2013).
[17]A. Sommerfeld, Math. Ann. **47**, 317 (I896).
[18]J. B. Keller, IRE Trans. Antennas Propag. **8**, 175 (1960).
[19]V. M. Sundaram and S.-b. Wen, Opt. Lett. **39**, 582 (2014).
[20]A. F. Stevenson, J. Appl. Phys. **24**, 1134 (1953).
[21]Y. Luo, J. B. Pendry, and A. Aubry, Nano Lett. **10**, 4186 (2010).
[22]S. K. Thamida and H.-C. Chang, Phys. Fluids **14**, 4315 (2002).
[23]R. Zhou, P. Wang, and H.-C. Chang, Electrophoresis **27**(7), 1376 (2006).
[24]S. Basuray, S. Senapati, A. Aijian, A. R. Mahon, and H.-C. Chang, ACS Nano **3**, 1823 (2009).
[25]See supplementary material at http://dx.doi.org/10.1063/1.4869694 for fabrication methods, materials and imaging analysis.
[26]I.-F. Cheng, S. Senapati, X. Cheng, S. Basuray, and H.-C. Chang, Lab Chip **10**, 828 (2010).